Annals of Forest Science (2021) 78: 77
https://doi.org/10.1007/s13595-021-01092-x

RESEARCH PAPER

Predicting crown width and length using nonlinear mixed-effects models: a test of competition measures using Chinese fir (*Cunninghamia lanceolata* (Lamb.) Hook.)

Wenwen Wang[1] · Fangxing Ge[1,2] · Zhengyang Hou[1] · Jinghui Meng[1]

Received: 17 May 2021 / Accepted: 27 July 2021 / Published online: 6 September 2021

Abstract

Key message **Including individual-tree competition indices as predictor variables could significantly improve the performance of crown width and length models for Chinese fir (*Cunninghamia lanceolata* (Lamb.) Hook.). Moreover, distance-dependent competition indices are superior to distance-independent ones when modeling crown width and length. Compared with crown width and length basic models with optimum competition indices, the performance of the two-level nonlinear mixed-effects models improved.**

Context Crown width (CW) and crown length (CL) are two important variables widely included as the predictors in growth and yield models that contribute to forest management strategies.

Aims Individual-tree crown width and length models were developed with data from 1498 Chinese fir (*Cunninghamia lanceolata* (Lamb.) Hook.) trees in 16 sample plots located at Jiangle County, Fujian Province, southeastern China. Two hypotheses were proposed: (1) including individual-tree competition indices as predictor variables could significantly improve performance of both the CW—DBH and CL—DBH models; and (2) the distance-dependent competition indices would perform better than distance-independent ones.

Methods The models were fitted using generalized linear least squares or generalized nonlinear least squares methods. In addition, to prevent correlations between observations from the same sampling unit, we introduced age classes and sample plots as random effects to develop the two-level nonlinear mixed-effects models.

Results We found introduction of competition indices could significantly improve the performance of the CW—DBH and CL—DBH models. The distance-dependent competition index (i.e., competitor to subject tree distance) performed best in modeling the crown width and length models. Compared with crown width and length basic models with optimum competition indices, the performance of the two-level nonlinear mixed-effects models was significantly better.

Conclusion The two hypotheses were accepted. We hope these models will contribute to scientific management of Chinese fir plantations.

Keywords Crown width and length models · Individual-tree competition indices · Optimum competition indices · Heteroskedasticity · Two-level nonlinear mixed-effects model

Handling Editor: Celine Meredieu

Contributions of the co-authors

All authors made significant contributions to the manuscript: Jinghui Meng and Zhengyang Hou conceived, designed and performed the experiments; Wenwen Wang and Fangxing Ge analyzed the data and results; Jinghui Meng, Wenwen Wang and Fangxing Ge are the main authors who developed and revised the manuscript.

Wenwen Wang and Fangxing Ge have contributed equally to this work and should be considered co-first authors.

Extended author information available on the last page of the article

1 Introduction

Forests are the largest territorial ecosystems on Earth and provide myriad ecosystem services (Buschbacher 1990; Meng et al. 2016b). Generally, ecosystem structure determines function (Warfield 2006), as is the case for forests (Meng et al. 2016a). Canopy structure plays a vital role in shaping forest ecosystems because it serves as a major layer for photosynthesis, respiration, and transpiration (Hernandezmoreno et al. 2017; Wang and Jarvis 1990). Additionally, canopy structure plays a dominant role in regulating energy

flow processes, and hence has an important effect on tree growth, dynamics, and productivity (Geißler et al. 2013; Leiterer et al. 2015).

Individual-tree crowns are the basic unit of forest canopy structure (Mallinis et al. 2013). Tree crown is an explicit and direct indicator describing tree vigor and health (Zarnoch et al. 2004), long-term competitiveness (Biging and Dobbertin 1992), productivity (Stenberg et al. 1994), and wood quality (De Kort et al. 1991). It is also extensively used to estimate individual-tree growth (Leites et al. 2009), individual-tree aboveground biomass (Carvalho and Parresol 2003), crown light interception (Pukkala et al. 1991), crown fire risk (Gómez-Vázquez et al. 2014), and stand regeneration (Crookston and Stage 1999). However, labor- and time-intensive measurement of tree crowns impairs its wide application to inform forest management. As such, a number of studies have focused on developing individual crown models (Sharma et al. 2016). Crown models have been widely integrated into individual-tree-based stand simulators, such as Forest Vegetation Simulator (FVS) (Johnson 1997), SILVA (Pretzsch et al. 2006), BWINPro (Nagel and Schmidt 2006), and FORest of RUSsia – Stand (FOR-RUS – S) (Chumachenko et al. 2003), which have facilitated forest management decision making.

Crown width (CW) and crown length (CL) are two important features of tree crown structure (Zeng 2015). These two features are often predicted using diameter at breast height (DBH) as the independent variable with linear or nonlinear regression (Russell and Weiskittel 2011). The regression methods require the following assumptions (Ritz and Streibig 2008; Sheather 2009): (1) errors e_1, e_2, …, e_n are independent; (2) errors e_1, e_2, …, e_n have a common variance σ^2; and (3) the errors are normally distributed with a mean of 0 and variance σ^2, that is, $e|X \sim N(0, \sigma^2)$. However, forestry data typically are spatially and temporally auto-correlated (Grégoire et al. 1995). The above assumptions could be violated due to the hierarchical and longitudinal structure of forestry data, resulting in biased estimation of standard error of parameters (Calama and Montero 2004; Fu et al. 2013). Because mixed-effects models provide a flexible and powerful tool for analysis of grouped data (e.g., longitudinal data, repeated measures data, blocked designs data, and multilevel data) (Zhao et al. 2013), many authors (Lindstrom and Bates 1990; Vonesh and Chinchilli 1997) have employed it to predict tree crown variables and found that this approach outperformed conventional regression methods (Fu et al. 2013; Sharma et al. 2016). For example, Sharma et al. (2016) and Sánchez-González et al. (2007) introduced sample plot as a random effect into basic CW—DBH functions. Fu et al. (2013) incorporated both site index class and sample plot as random effects into their basic CW—DBH function. Fu et al. (2017) added both block and sample plot as random effects into a basic height to crown base (HCB)—DBH function.

Differing from open-grown trees, the crown width and length for stand-grown trees is significantly influenced by competition among individual trees (Pacala et al. 1996; Sharma et al. 2016). Individual-tree competition indices (CIs), which can be classified into distance-dependent CIs and distance-independent CIs, have been being developed since the 1960s to quantify individual-tree-level competition (Schröder and Gadow 1999; Stadt et al. 2002). Unfortunately, only a few studies on crown width and length models that include distance-dependent CIs (Davies and Pommerening 2008; Purves et al. 2007; Rüdiger 2003; Rouvinen and Kuuluvainen 1997; Thorpe et al. 2010), and fewer researchers compared the performance of distance-dependent CIs and distance-independent CIs in developing crown models (Sharma et al. 2016).

In the present study, we hypothesized that including CIs as predictor variables could significantly improve performance of both CW—DBH and CL—DBH models. Moreover, since spatial arrangement of trees could have a significant influence on their growth (Pukkala and Kolstroem 1991), we proposed a second hypothesis that distance-dependent CIs perform better than distance-independent CIs. The objectives of this present study were (1) to test the hypotheses by including both distance-dependent and distance-independent CIs for development of CW and CL models, (2) identify the optimum CIs for the models, and (3) produce mixed-effects predictive models for CW and CL using optimum CIs for a Chinese fir plantation.

2 Materials and methods

2.1 Study area

Our study area was located in Jiangle County (26° 26′ N to 27° 04′ N, 117° 05′ E to 117° 40′ E) in Fujian Province, southeastern China. It has a subtropical monsoon climate with characteristics of both an oceanic and continental climate. The annual average temperature is 18.7 °C, the annual average precipitation is 1698.2 mm, the annual average sunshine time is 1730 h, and the average frost-free period is 295 days (Lin et al. 2018). The main soil type in the study area is red soil. Hills and low mountains are the main landforms, accounting for 90% of the region. The average elevation is 540 m, with the highest peak 1620 m. The main vegetation types include natural secondary forest, Chinese fir plantations, and Masson pine (*Pinus massoniana* Lamb.) plantations (Chen et al. 2018).

2.2 Data source

Data employed in this study were collected from 16 squared sample plots of 400 m^2 in even-aged, pure Chinese fir

plantations. *C. lanceolata* accounted for 97.73% of total basal area in this plantation, with the other 2.27% represented by 15 tree species, e.g., *Cinnamomum camphora* (L.) Presl (0.73%), *Vernicia montana* Lour. (0.36%), and *Magnolia officinalis* Rehd. et Wils. (0.20%). These 16 sample plots were further grouped into the following categories based on age classes: 4 sample plots of young stands (6 years), 4 sample plots of middle-aged stands (16 years), 4 sample plots of near mature stands (23 years), and 4 sample plots of mature stands (30 years).

For each standing live tree, DBH and relative coordinates were measured with a precision of 0.1 cm and 0.01 m, respectively. Using a Vertex III altimeter (Vasilescu 2013), total tree heights (*H*) and height to crown base (HCB) were measured with a precision of 0.1 m. CW was calculated as the arithmetic mean of two crown widths, derived from the four measured crown radii at two azimuths. The first azimuth was defined as the direction from the subject tree to the center of the sample plot, and the second azimuth was perpendicular to the first (Marshall et al. 2003; Sharma et al. 2016). The number of trees measured was 1565, including 1498 Chinese fir and 67 broad-leaved trees. These 1565 trees were used to derive competition indices for each individual tree (but CW and CL models were fitted using the 1498 Chinese fir trees). The descriptive statistics for the 1498 Chinese fir trees are summarized in Table 1.

Table 1 Descriptive statistics of Chinese fir trees ($n = 1498$)

Variable	Min	Max	Mean	SD	C_v%
DBH (cm)	4.0	38.8	14.44	5.36	37.08
H (m)	3.5	32.2	12.91	5.49	42.55
A (yr)	6	30	16.52	8.42	54.27
CW (m)	0.3	5.2	2.50	0.78	31.04
CL (m)	0.1	22.3	4.66	2.33	50.09
HCB (m)	2.1	24.7	8.25	4.24	51.36
TPH (trees·ha^{-1})	1159	3136	2217.00	639.56	28.85

Min, minimum; *Max*, maximum; *SD*, standard deviation; *Cv%*, coefficient of variation; *DBH*, diameter at breast height; *H,* height; *A*, stand age; *CW*, crown width; *CL*, crown length; *HCB*, height to crown base; *TPH*, trees per hectare

2.3 Methods

2.3.1 Basic model selection

The ten functions provided in Table 2 were selected as candidate basic models for the CW—DBH and CL—DBH relationships for individual trees (Sánchez-González et al. 2007; Sönmez 2009).

The candidate basic models were fitted using generalized linear least squares (GLS) or generalized nonlinear least squares (GNLS) method with *gls* or *gnls* function in the nlme package of R software (Pinheiro et al. 2012; R Team RDC 2013). For model evaluation, the lack-of-fit test statistics, i.e., −2 log-likelihood (−2LL), Akaike information criterion (AIC), Bayesian information criterion (BIC), absolute bias (Bias), root mean square error (RMSE), and coefficient of determination (R^2), were calculated.

Additionally, the predictive performance of models was further validated using the ten-fold cross-validation procedure by calculating normalized mean square error for the test set (NMSE) (Levi et al. 2015) and predicted the error sum of squares (PRESS) (Quan 1988). The formulas were as follows:

$$\mathrm{NMSE} = \overline{(y_j - \hat{y}_j)^2} / \overline{(y_j - \overline{y_j})^2} = \frac{\sum (y_j - \hat{y}_j)^2}{\sum (y_j - \overline{y_j})^2} \quad (1)$$

$$\mathrm{PRESS} = \sum_{j=1}^{n} (y_j - \hat{y}_j)^2 \quad (2)$$

Table 2 Crown width or length basic models considered in the present study

Function no	Function	Function form	Reference
[CR1]	$CR = \phi_1 + \phi_2 DBH$	Linear	Sánchez-González et al. (2007), Sönmez (2009), Buba (2013)
[CR2]	$CR = \phi_1 + \phi_2 DBH + \phi_3 DBH^2$	Quadratic	Sánchez-González et al. (2007), Sönmez (2009), Martin et al. (2012)
[CR3]	$CR = \phi_1 + \phi_2 DBH + \phi_3 DBH^2 + \phi_4 DBH^3$	Cubic	Sönmez (2009)
[CR4]	$CR = \phi_1 DBH^{\phi_2}$	Power	Sánchez-González et al. (2007), Sönmez (2009)
[CR5]	$CR = \phi_1 [1 - \exp(-\phi_2 DBH)]$	Monomolecular	Sánchez-González et al. (2007)
[CR6]	$CR = [DBH/(\phi_1 + \phi_2 DBH)]^2$	Hossfeld	Sánchez-González et al. (2007)
[CR7]	$CR = \phi_1 (\phi_2)^{DBH}$	Compound	Sönmez (2009)
[CR8]	$CR = \exp(\phi_1 + \phi_2 DBH)$	Growth	Sönmez (2009)
[CR9]	$CR = \phi_1 \exp(\phi_2 DBH)$	Exponential	Sönmez (2009)
[CR10]	$CR = \phi_1 / [1 + \phi_2 \exp(-\phi_3 DBH)]$	Logistic	Fu et al. (2013)

CR, crown width or length; *DBH*, diameter at breast height; ϕ_1, ϕ_2, and ϕ_3: formal parameters

where y_j is the jth observed value in the test set, $\widehat{y}_j$ is the jth value predicted from y_j by the model fitted by the training set, and $\overline{y_j}$ is the mean of the observed values in the test set.

Based on model evaluation and validation, the final optimum basic model was determined.

2.3.2 Competition indices calculation

Ten candidate competition indices including four distance-independent indices and six distance-dependent indices (Table 3) were compared for their performance in predicting crown width and length.

To calculate the competition indices, we classified trees in the sample plots into subject trees and competitor trees. Each and every tree needs be treated as both types for given data quality and amounts. Identifying competitor trees are of great importance to derive competition indices. However, competitor searching methods vary among different studies (Bella 1971; Pommerening 2008; Wang et al. 2016). Among these methods, four neighboring trees proposed by Hui and Gadow (Hui and Gadow 2003) (four neighboring trees as competitors in four different directions around the subject tree) and fixed radii (all neighboring trees as competitors around the subject trees lying around a search radius with 3.5 times the mean crown radius of canopy trees) (Mailly et al. 2003) have been extensively employed. In the data pre-analysis, we applied these two methods and found that fixed radii worked better, which is also consistent with Lorimer (1983) who recommends such a rule for most applications. In the present study, we selected the second method to search competitors.

Subject trees near sample plot edges may have competitor trees that are out of the sample plot. These are edge effects, which could bring errors into estimation of competition indices (Tang et al. 2007). We employed toroidal edge correction (also referred to as translation) to reduce such edge effects. For each sample plot, make 8 copies of the original sample plot, then one of the copies is moved from original position into up, down, left, right, upper left, lower left, lower right, and upper right direction, respectively. So a new bigger sample plot consisted of 9 original is created (Fig. 1). When calculating individual competition indices, subject trees are defined as individuals located in original sample plot (Haase 1995; Pommerening and Stoyan 2006; Diggle 2013). Scatters distribution of crown width or length and calculated CIs showed that competitions have a significant effect on the growth of crown width and length (Figs. 2, 3).

2.3.3 Optimum competition index identification

To determine the optimum competition index and its optimum position, each competition index was added independently with different positions to the basic model determined in Basic model selection section. Following

Table 3 List of candidate competition indices

Index	Abbreviation	Formula
Distance-independent indices		
Sum of the diameters of the competitors (Steneker and Jarivis 1963)	SDBH	$\sum_{j=1}^{n} \mathrm{D}_j$
Sum of the basal areas of the competitors (Steneker and Jarivis 1963)	SBA	$\sum_{j=1}^{n} \mathrm{BA}_j$
Competitor to subject tree diameter (Lorimer 1983)	CSDBH	$\frac{\sum_{j=1}^{n} D_j}{D_i}$
Subject tree to competitor basal area (Daniels et al. 1986)	SCBA	$\frac{{D_i}^2}{n \cdot \sum_{j=1}^{n} {D_j}^2}$
Distance-dependent indices		
Hegyi (1974)	Heygi	$\sum_{j=1}^{n} \left(\frac{D_j}{D_i} \cdot \frac{1}{\mathrm{DIST}_{ij}} \right)$
Alemdag (1978)	Alem	$\sum_{j=1}^{n} \left\{ \pi \cdot \left[\frac{D_i \bullet \mathrm{DIST}_{ij}}{D_i + D_j} \right]^2 \cdot \left[\frac{D_j / \mathrm{DIST}_{ij}}{\sum_{j=1}^{n} (D_j / \mathrm{DIST}_{ij})} \right] \right\}$
Johann (1982)	Joha	$\sum_{j=1}^{n} \left(\frac{H_i}{\mathrm{DIST}_{ij}} \cdot \frac{D_j}{D_i} \right)$
Open Comparison (Hu 2010)	OP	$\mathrm{OP} = \frac{1}{4} \sum_{j=1}^{n} t_{ij}$; $t_{ij} = \begin{cases} 1, \text{if } \mathrm{DIST}_{ij} \geq H_j - H_i \\ 0, \text{if } DIST_{ij} < H_j - H_i \end{cases}$
Martin and Ek (1984)	MaEk	$\sum_{j=1}^{n} \frac{D_j}{D_i} \cdot \exp\left[-\frac{16 \cdot \mathrm{DIST}_{ij}}{D_i + D_j} \right]$
Jiang and Qiu (1994)	JiQi	$\frac{D_i}{\frac{1}{n} \sum_{j=1}^{n} D_j} \cdot \frac{1}{n} \sum_{j=1}^{n} \mathrm{DIST}_{ij}$

D_i, diameter at breast height of subject tree i; D_j, diameter at breast height of competitor tree j; H_i, height of subject tree i; H_j, height of competitor tree j; $DIST_{ij}$, distance between subject tree i and competitor j; BA_j, basal area of competitor tree j

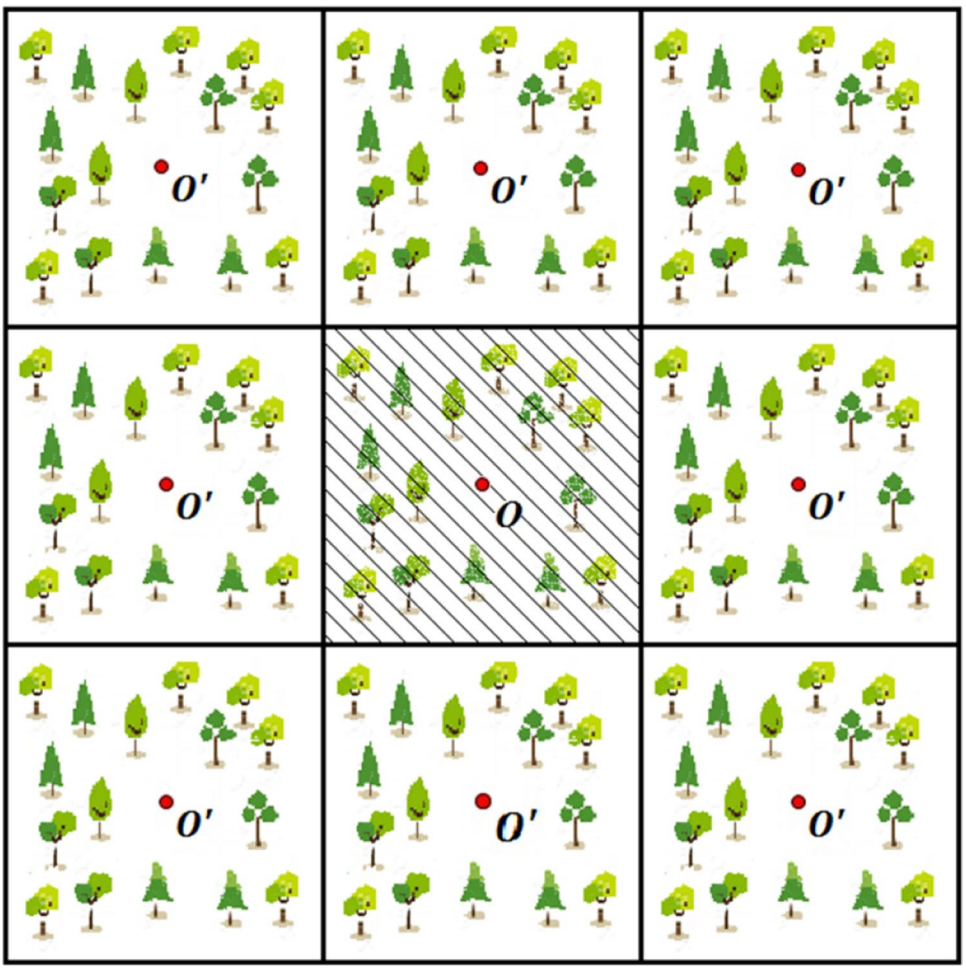

Fig. 1 Illustration of the translation edge-correction methods used in this study

Schröder and Gadow (1999) and Mailly et al. (2003), we calculated the mean square error reduction (MSER) relative to a no competition index to identify the optimum combination of the competition index and its position for the crown width or length models. The formula of MSER was as follows:

$$\mathrm{MSER} = \left(1 - \frac{\mathrm{MSE}_2}{\mathrm{MSE}_1}\right) \times 100 \tag{3}$$

where MSE_1 is the mean square error of the basic crown width or crown length model and MSE_2 is the mean square error of the models after adding the competition index.

For the CW—DBH and CL—DBH relationships, the optimum basic models determined in basic model selection section, and the optimum combination of competition indices and their positions identified in this section, were then employed as our final basic model, based on which the mixed-effects crown width or length models were further developed.

2.3.4 Two-level nonlinear mixed-effects models

General model form Due to hierarchical structure of data (i.e., trees within a sample plot, and sample plots within an age class), we introduced two-level random effects to our basic model. The first-level random effect is age class, and sample plot (nested in age classes) serves as the second-level random effect.

The formulas of two-level linear or nonlinear mixed-effects models can be expressed as follows:

$$\begin{gathered} y_{ijk} = f\left(\varphi_{ijk}, t_{ijk}\right) + \varepsilon_{ijk}, i = 1, \ldots, M, j = 1, \ldots, M_i; k = 1, \ldots, n_{ij} \\ \varepsilon_{ijk} \sim N(0, \sigma^2 R_{ij}) \end{gathered} \tag{4}$$

where y_{ijk} denotes a response value of the kth observation (tree) on the jth group (sample plot) nested within-group i (age class). M is the number of first-level groups, M_i is the number of second-level groups within-group i, n_{ij} is the

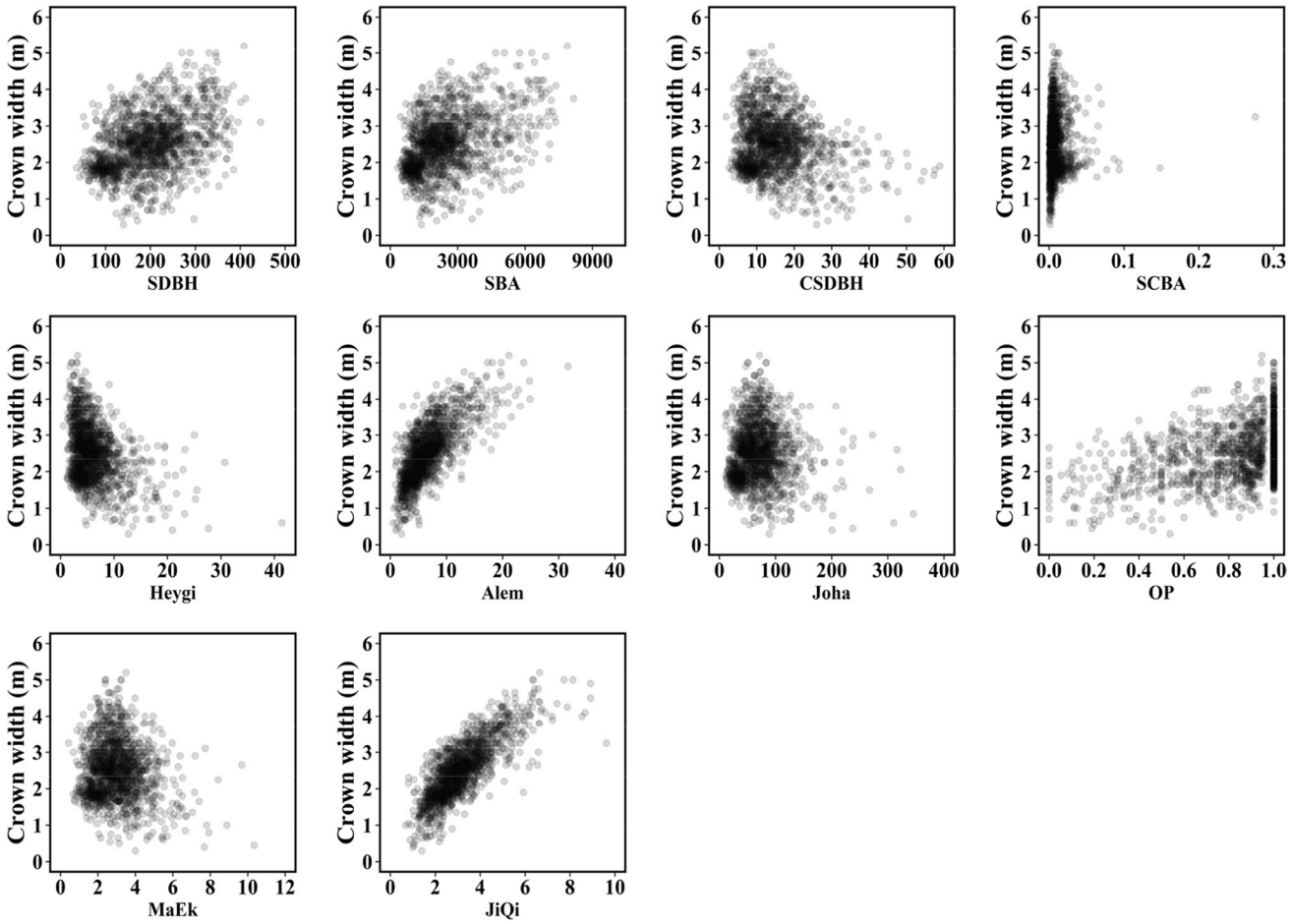

Fig. 2 Scattered plots of crown width against different competition indices, respectively

number of observations on the *j*th group in group *i*; $f(\cdot)$ is a general, real-valued, differentiable function of a group-specific parameter vector φ_{ijk} and a covariate vector t_{ijk}. The within-group error ε_{ijk}, which contains within-group variance and correlation, is assumed to be normally distributed with zero expectation and a positive-definite variance–covariance structure R_{ij}, generally expressed as a function of the parameter vector λ (Fu et al. 2013).

The φ_{ijk} can be further written as follows:

$$\varphi_{ijk} = A_{ijk}\beta + B_{i,jk}\mu_i + M_{ijk}\mu_{ij},\ \mu_i \sim N\left(0, \psi_1\right), \mu_{ij} \sim N(0, \psi_2) \tag{5}$$

where β is a p-dimensional vector of fixed effects. μ_i and μ_{ij} are the first and second random effects, which are independent and normally distributed q_1- and q_2-dimensional vectors with zero mean and respective variance–covariance matrices ψ_1 and ψ_2. A_{ijk}, $B_{i,jk}$, and M_{ijk} are design matrices. μ_i, μ_{ij}, and ε_{ijk} are mutually independent. The variance–covariance matrices of ψ_1 and ψ_2 were assumed to be unstructured.

Determining parameter effects In this study, all possible combinations of random effects were fitted and then the best combination was selected according to lack-of-fit statistics, i.e., −2LL, AIC, BIC, and likelihood ratio test (L.Ratio).

Determining the matrix of R_{ij} Forestry data often exhibit autocorrelation and heteroskedasticity (Gregorie 1987), which results in incorrect standard errors and estimation intervals. Therefore, within-group variance and autocorrelation structure in R_{ij} should be specified (Davidian 2017; Meng and Huang 2009). The following within-group variance–covariance matrix (Davidian 2017; Zhao et al. 2013) is usually used:

$$R_{ij} = \sigma^2 G_{ij}^{0.5} \Gamma_{ij} G_{ij}^{0.5} \tag{6}$$

where σ^2 is a scaling factor that is equal to residual variance of the developed model, G_{ij} is a diagonal matrix which

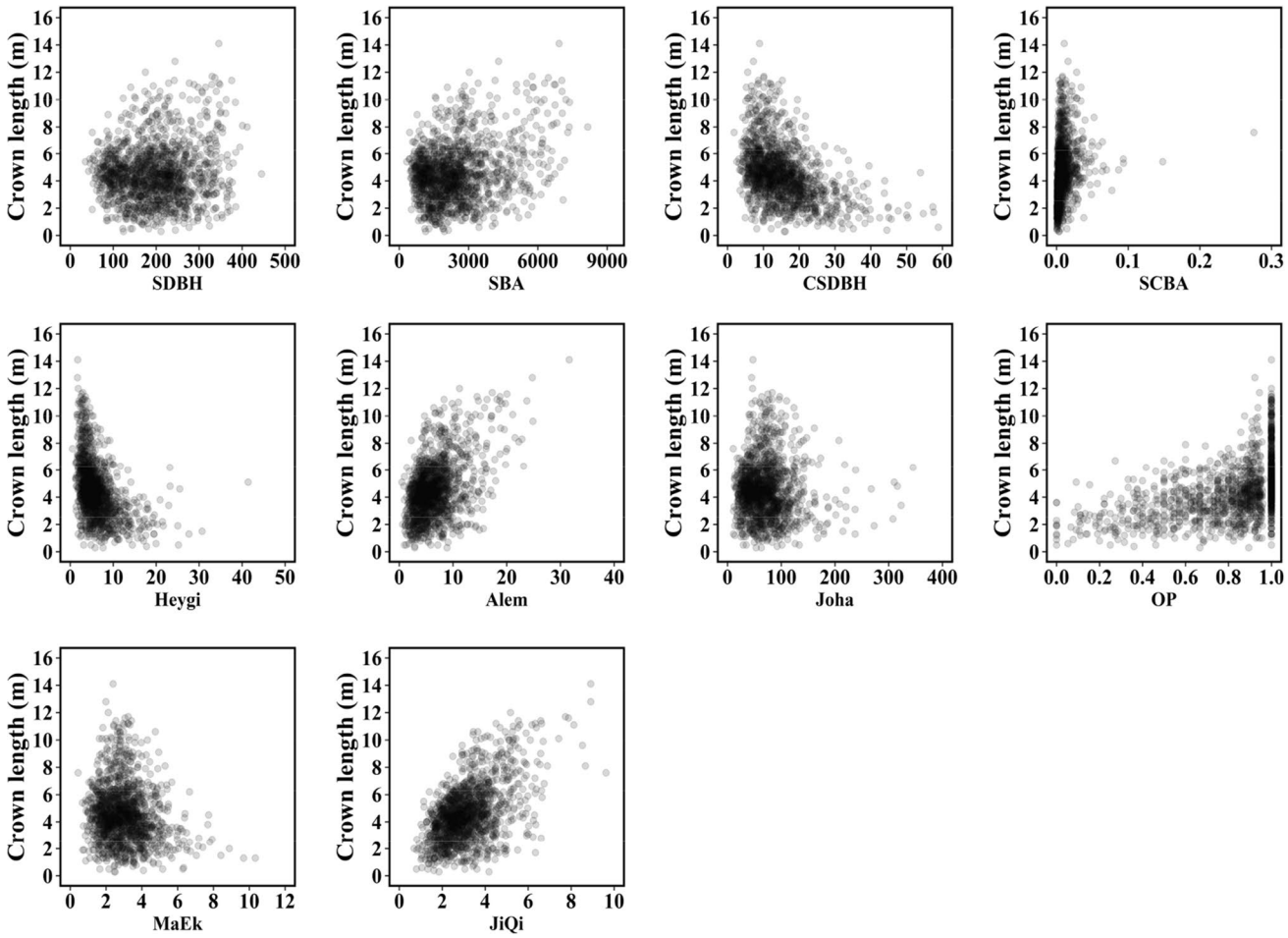

Fig. 3 Scattered plots of crown length against different competition indices, respectively

describes heteroscedasticity, and Γ_{ij} is a matrix showing the autocorrelation structure of errors.

Because our data are only from one measurement period, autocorrelation was not considered. Therefore, Γ_{ij} reduced to a $n_{ij} \times n_{ij}$ identity matrix, and three variance functions, i.e., the exponential function [Eq. (7)], the power function [Eq. (8)] and the constant plus power function [Eq. (9)], were used to reduce heteroscedasticity (Wang et al. 2019; Zhao et al. 2013).

$$\mathrm{varExp}(\varepsilon_{ijk}) = \sigma^2 \exp(2\alpha u_{ijk}) \tag{7}$$

$$\mathrm{varPower}(\varepsilon_{ijk}) = \sigma^2 \exp(u_{ijk}^{2\alpha}) \tag{8}$$

$$\mathrm{varConstPower}(\varepsilon_{ijk}) = \sigma^2 (\alpha + u_{ijk}^{\beta})^2 \tag{9}$$

where u_{ijk} is the estimated value based on fixed parameters of the mixed-effects models and α and β are estimated parameters of variance functions.

Model prediction and evaluation The final produced mixed-effects models for crown width and length with optimum competition indices were evaluated for their predictive performance. We performed a tenfold cross-validation procedure and NMSE and PRESS were calculated. In addition, likelihood ratio tests were conducted among the optimum basic model, optimum basic model with the best CI, and the optimum mixed-effects models for the CW and CL.

3 Results

3.1 Determination of basic models

The lack-of-fit statistics of the candidate CW and CL models are summarized in Tables 4 and 5, respectively. Although the lack-of-fit statistics were almost identical for most of the functions, the function [CR4] (cubic form) showed a slightly better performance for both the crown width and length. NMSE and PRESS produced by the tenfold cross-validation also indicated slightly better

Table 4 Lack-of-fit statistics for CW—DBH basic models

Function no	Fitting statistics of the candidate crown width models						Cross-validation	
	−2LL (df)	AIC	BIC	Bias (m)	RMSE (m)	R^2	NMSE	PRESS
[CR1][b]	2576.04 (3)	2582	2598	0.00	0.57	0.4566	0.5535	48.7260
[CR2][c]	2585.43 (4)	2593	2615	0.00	0.57	0.4584	0.5525	48.6443
[CR3][c]	2595.93 (5)	2606	2632	0.00	0.57	0.4613	0.5508	48.5197
[CR4][b]	2552.41 (3)	2558	2574	0.00	0.57	0.4623	0.5505	48.4941
[CR5][b]	2584.56 (3)	2591	2606	0.01	0.58	0.5021	0.5623	49.5767
[CR6][b]	2597.36 (3)	2603	2619	0.00	0.58	0.4823	0.5667	49.9972
[CR7][b]	2601.31 (3)	2607	2623	−0.00	0.58	0.4176	0.5699	50.1528
[CR8][b]	2601.31 (3)	2607	2623	−0.00	0.58	0.4176	0.5617	50.0737
[CR9][b]	2601.31 (3)	2607	2623	−0.00	0.58	0.4176	0.5680	50.1595
[CR10][b]	2563.32 (4)	2571	2593	−0.00	0.57	0.4490	0.5560	48.9412

CR, crown width; *−2LL (df)*, −2 log-likelihood (degree of freedom); *AIC*, Akaike information criterion; *BIC*, Bayesian information criterion; *Bias*, absolute bias; *RMSE*, root mean square error; R^2, coefficient of determination; *NMSE*, normalized mean square error; *PRESS*, predicted the error sum of squares

[b]*P* value for each coefficient is lower than 0.05 in a *T*-test

[c]*P* values for one or more than one coefficient are higher than 0.05 in a *T*-test

Table 5 Lack-of-fit statistics for CL—DBH basic models

Function no	Fitting statistics of the candidate crown length models						Cross-validation	
	−2LL (df)	AIC	BIC	Bias (m)	RMSE (m)	R^2	NMSE	PRESS
[CR1][b]	5353.92 (3)	5360	5376	0.00	1.49	0.4772	0.5319	332.3461
[CR2][c]	5362.14 (4)	5370	5391	0.00	1.49	0.4786	0.5315	331.9982
[CR3][c]	5376.44 (5)	5386	5413	0.00	1.49	0.4794	0.5316	331.9573
[CR4][b]	5346.14 (3)	5352	5368	0.01	1.50	0.4903	0.5302	332.3337
[CR5][b]	5353.00 (3)	5359	5375	0.02	1.50	0.5139	0.5359	334.8563
[CR6][b]	5392.51 (3)	5399	5414	0.03	1.52	0.5153	0.5493	343.4263
[CR7][b]	5366.53 (3)	5373	5388	−0.01	1.51	0.4412	0.5435	339.3601
[CR8][b]	5366.53 (3)	5373	5388	−0.01	1.51	0.4412	0.5441	338.1158
[CR9][b]	5366.53 (3)	5373	5388	−0.01	1.51	0.4412	0.5435	339.3601
[CR10][b]	5343.36 (4)	5351	5373	−0.00	1.50	0.4707	0.5339	333.5384

CR, crown length; *−2LL(df)*, −2 log-likelihood (degree of freedom); *AIC*, Akaike information criterion; *BIC*, Bayesian information criterion; *Bias*, absolute bias; *RMSE*, root mean square error; R^2, coefficient of determination; *NMSE*, normalized mean square error; *PRESS*, predicted the error sum of squares

[b]*P* value for each coefficient is lower than 0.05 in a *T*-test

[c]*P* values for one or more than one coefficient are higher than 0.05 in a *T*-test

performance for the function [CR4]. Moreover, the scattered plots of the CW or CL against DBH (Fig. 4) were suitfully fitted by the function [CR4]. Therefore, this function was selected as the basic model for modeling the CW—DBH and CL—DBH relationships. The optimum basic models are as follows:

$$CW_{ijk} = 0.5403 DBH_{ijk}^{0.5794} + \varepsilon_{ijk} \quad (10)$$

$$CL_{ijk} = 0.4356 DBH_{ijk}^{0.8829} + \varepsilon_{ijk} \quad (11)$$

where CW_{ijk}, CL_{ijk}, and DBH_{ijk} are crown width, crown length, and diameter at breast height, respectively, of the *k*th tree in the *j*th plot in the *i*th age class; ε_{ijk} is a model error term.

3.2 Inclusion of competition index

Based on Eq. (10) and Eq. (11), effects of adding different competition indices at varying positions on the improvement of CW—DBH and CL—DBH models were compared (Tables 6 and 7).

In terms of the CW—DBH model, it can be seen from Table 6 that JiQi has the largest MSER of 32.38, but it was not selected since its insignificant coefficient. Therefore, the Alem was identified as the optimum

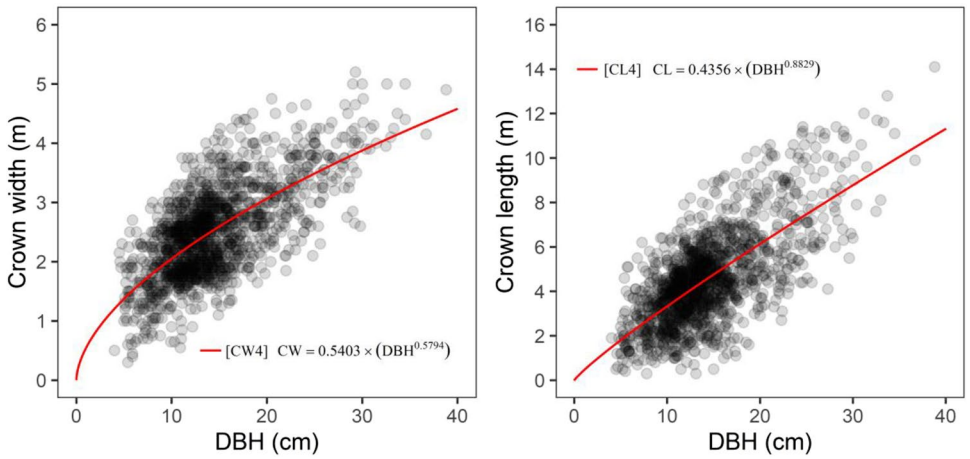

Fig. 4 Scattered plots of crown width or length against DBH for [CR4], respectively

Table 6 Comparison of different competition indices added to the CW—DBH basic model [CW4]

CI no	$CW=(\phi_1+\phi_3 CI)DBH^{\phi 2}$			$CW=\phi_1 DBH^{(\phi 2+\phi 3CI)}$		
	Adjust R^2	MSE	MSER (%)	Adjust R^2	MSE	MSER (%)
None						
SDBH	0.5091	0.2905	10.63[b,d]	0.5000	0.2936	9.68[b]
SBA	0.4653	0.3196	1.70[b]	0.4638	0.3201	1.54[b]
CSDBH	0.5115	0.2908	10.55[b]	0.5128	0.2898	10.87[b,d]
SCBA	0.4756	0.3127	3.80[b]	0.4913	0.3095	4.81[b]
Heygi	0.4715	0.3174	2.35[b]	0.4738	0.3165	2.63[b]
Alem	0.5517	0.2586	20.44[b,d]	0.4883	0.2839	12.67[b]
Joha	0.4620	0.3243	0.23[c]	0.4621	0.3243	0.23[c]
OP	0.4852	0.3145	3.24[b]	0.4816	0.3140	3.41[b]
MaEk	0.4619	0.3250	0.02[c]	0.4617	0.3250	0.01[c]
JiQi	0.6329	0.2198	32.38[c]	0.5048	0.2669	17.89[b,d]

CW, crown width; *CI*, competition index; *DBH*, diameter at breast height; ϕ_1, ϕ_2 and ϕ_3: formal parameters; *Adjust* R^2, adjusted coefficient of determination; *MSE*, mean square error; *MSER (%)*, mean square error reduction (%) relative to the regression model with no competition index

[b] *P* values for ϕ_1, ϕ_2, and ϕ_3 are lower than 0.05 in a *T*-test

[c] *P* value for one or more than one coefficient are higher than 0.05 in a *T*-test

[d] Superior competition index selected from the two categories of CIs

competition index since it yielded the second largest MSER of 20.44. The corresponding model form was written as:

$$CW_{ijk} = (0.9533+0.0516\text{Alem})DBH_{ijk}^{0.2474} + \varepsilon_{ijk} \quad (12)$$

Regarding crown length, the OP exhibited a better performance than the other competition indices with the largest MSER of 14.31 (Table 7). The corresponding model form was as follows:

$$CL_{ijk} = 0.5991DBH_{ijk}^{(0.5122+0.2897OP_{ijk})} + \varepsilon_{ijk} \quad (13)$$

where $JiQi_{ijk}$ and OP_{ijk} are JiQi and OP, respectively, of the *k*th tree in the *j*th sample plot in the *i*th age class.

In addition, the CW and CL curves overlaid on the measured data (DBH and the optimum competition index, i.e., Alem and OP) were presented in Fig. 5, which showed that the scattered plots were suitfully fitted by the Eqs. (12–13).

3.3 Development of the two-level mixed-effects model

There are 49 ($C_3^1C_3^1 + C_2^1C_3^2C_3^1 + C_2^1C_3^3C_3^1 + C_3^2C_3^2 + C_2^1C_3^2C_3^3 + C_3^3C_3^3 = 49$) potential combinations of random effects for

Table 7 Comparison of different competition indices added to CL—DBH basic model [CL4]

CI no	$CL=(\phi_1+\phi_3 CI)DBH^{\phi 2}$			$CL=\phi_1 DBH^{(\phi 2+\phi 3 CI)}$		
	Adjust R^2	MSE	MSER (%)	Adjust R^2	MSE	MSER (%)
None						
SDBH	0.4919	2.2254	0.64[c]	0.4912	2.2311	0.39[c]
SBA	0.4916	2.2337	0.27[c]	0.4911	2.2373	0.11[c]
CSDBH	0.4994	2.2155	1.09[b,d]	0.4952	2.2143	1.14[b,d]
SCBA	0.4890	2.2373	0.11[c]	0.4890	2.2387	0.05[c]
Heygi	0.4952	2.2310	0.39[c]	0.4935	2.2269	0.58[c]
Alem	0.4899	2.2396	0.01[c]	0.4890	2.2394	0.02[c]
Joha	0.4918	2.2307	0.40[c]	0.4928	2.2290	0.48[c]
OP	0.5683	1.9607	12.46[b,d]	0.5724	1.9194	14.31[b,d]
MaEk	0.4927	2.2281	0.52[c]	0.4913	2.2296	0.46[c]
JiQi	0.4904	2.2386	0.05[c]	0.4894	2.2398	0.00[c]

CL, crown length; *CI*, competition index; *DBH*, diameter at breast height; ϕ_1, ϕ_2 and ϕ_3: formal parameters; *Adjust* R^2, adjusted coefficient of determination; *MSE*, mean square error; *MSER (%)*, mean square error reduction (%) relative to the regression model with no competition index

[b] *P* values for ϕ_1, ϕ_2, and ϕ_3 are lower than 0.05 in a *T*-test

[c] *P* value for one or more than one coefficient are higher than 0.05 in a *T*-test

[d] Superior competition index selected from the two categories of CIs

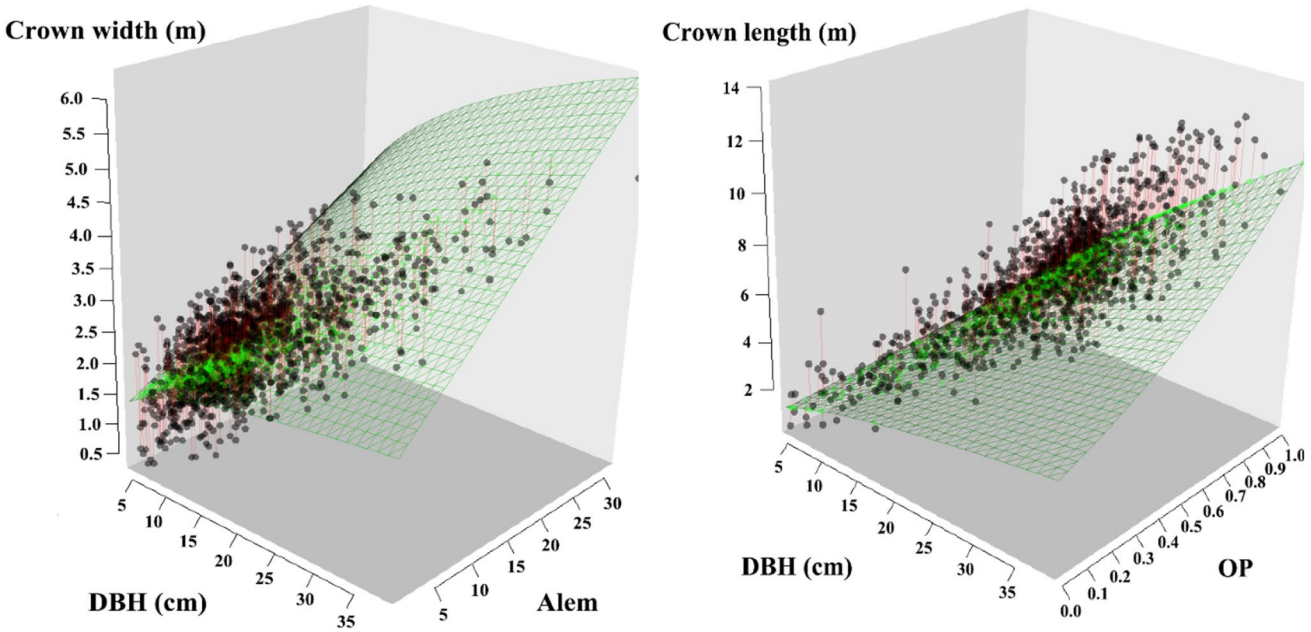

Fig. 5 Scattered plots of crown width or length against DBH and CI for Eqs. (12–13)

Eq. (12) when considering all independent variables and the intercept in the basic model. When fitted to the data, all combinations reached convergence. Among these 49 mixed-effects models, Eq. (14) yielded the smallest AIC (1571), BIC (1613) and − 2LL [1554.91 (8)]. In addition, the L.Ratio (L.Ratio = 105.72, $p < 0.0001$) also indicated the best performance of Eq. (14). Therefore, Eq. (14) was the resulting mixed-effects model.

$$CW_{ijk} = [(\phi_1 + u_{1ij}) + \phi_3 Alem_{ijk}]DBH_{ijk}^{\phi_2+u_{1i}+u_{2ij}} + \varepsilon_{ijk} \quad (14)$$

where ϕ_1–ϕ_3 are the fixed-effects parameters, u_{1i} is a random-effects parameter generated by age class for the CW model, and u_{1ij} and u_{2ij} are random-effects parameters generated by interaction of age class and sample plot for the CW model.

There are 49 ($C_3^1C_3^1 + C_2^1C_3^2C_3^1 + C_2^1C_3^3C_3^1 + C_3^2C_3^2 + C_2^1C_3^2C_3^3 + C_3^3C_3^3 = 49$) potential combinations of random effects for Eq. (13) when considering all independent variables and the intercept in the basic model. When fitted to the data, a total of 38 combinations reached convergence. Among these 38 mixed-effects models, Eq. (15) yielded the smallest AIC (4869), BIC (4912), and − 2LL [4853.39 (8)]. In addition, the L.Ratio (L.Ratio = 9.05, $p = 0.0108 < 0.05$) also indicated the best performance of Eq. (15). Therefore, Eq. (15) was the resulting mixed-effects model.

$$CL_{ijk} = (\phi_1 + v_{1ij})DBH^{[\phi_2 + v_{1i} + (\phi_3 + v_{2ij})OP]} + \varepsilon_{ijk} \quad (15)$$

where ϕ_1–ϕ_3 are fixed-effects parameters, v_{1i} is a random-effects parameter generated by age class for the CL model, and v_{1ij} and v_{2ij} are random-effects parameters generated by interaction of age class and sample plot for the CL model.

We used three variance functions to reduce the heteroscedasticity of the residuals and their performances were compared in terms of AIC, BIC, − 2LL, and L.Ratio. The results showed that the mixed-effects models with variance function exhibited better performance than the one without considering the variance function. Performance also differed among the mixed-effects models with different variance functions (Tables 8 and 9). According to AIC, BIC, − 2LL, and L.Ratio, the exponent function was determined as the best variance function for CW and CL models.

After the determination of parameter effects and error variance–covariance structure, the final forms of

Table 8 The lack-of-fit statistics of the crown width mixed-effects model using different variance functions

Model	Variance function	AIC	BIC	− 2LL (df)	L.Ratio	*p* value
(14)	None	1571	1613	1554.91 (8)		
(14.1)	ConstPower	1568	1621	1548.23 (10)	6.69[b]	0.0353
(14.2)	Power	1568	1615	1549.67 (9)	5.24[b]	0.0220
(14.3)	Exponent	1567	1614	1548.54 (9)	6.38[b]	0.0116

AIC, Akaike information criterion; *BIC*, Bayesian information criterion; *− 2LL (df)*, − 2 log-likelihood (degree of freedom). [b]*L.Ratio*, the value of likelihood ratio test, which was calculated with respect to model (14)

Table 9 The lack-of-fit statistics of the crown length mixed-effects model using different variance functions

Model	Variance function	AIC	BIC	− 2LL (df)	L.Ratio	*p* value
(15)	None	4869	4912	4853.39 (8)		
(15.1)	ConstPower	4817	4870	4796.61 (10)	56.78[c]	< 0.0001
(15.2)	Power	4817	4865	4799.06 (9)	54.33[c]	< 0.0001
(15.3)	Exponent	4798	4846	4780.25 (9)	73.15[c]	< 0.0001

AIC, Akaike information criterion; *BIC*, Bayesian information criterion; *− 2LL(df)*, − 2 log-likelihood (degree of freedom). [c]*L.Ratio*, the value of likelihood ratio test, which was calculated with respect to model (15)

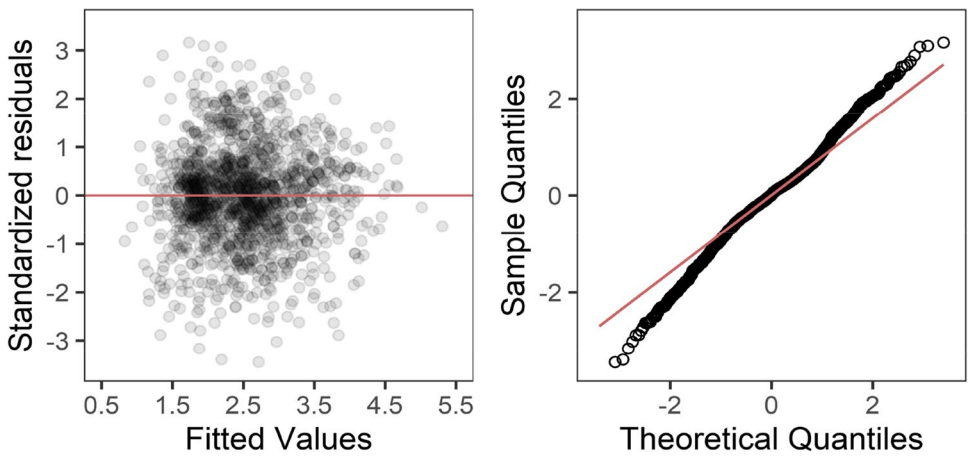

Fig. 6 Residual plot and QQ plot of the selected crown width mixed-effects model [Eq. (16)]

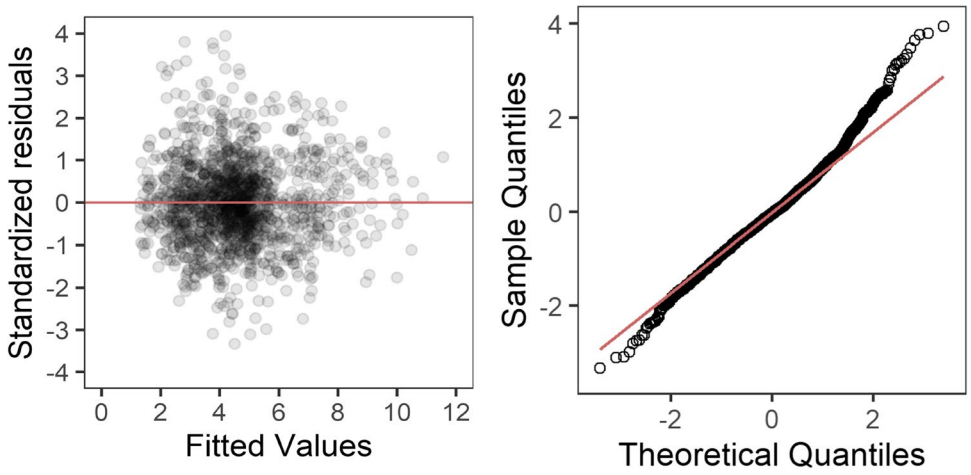

Fig. 7 Residual plot and QQ plot of the selected crown length mixed-effects model [Eq. (17)]

the CW and CL nonlinear mixed-effects models for Chinese fir in Fujian Province, southeastern China, were proposed in Eq. (16) and Eq. (17). The residual plots and QQ plots are shown in Figs. 6 and 7, respectively.

$$\mathrm{CW}_{ijk} = [(0.4229 + u_{1ij}) - (8.730e-4)\mathrm{Alem}_{ijk}]DBH_{ijk}^{0.7212+u_{1i}+u_{2ij}} + \varepsilon_{ijk} \quad (16)$$

where

$$u_i = \left[u_{1i}\right] \sim \mathrm{N}\{[0], \psi_i = (0.0014)\}$$
$$u_{ij} = \begin{bmatrix} u_{1ij} \\ u_{2ij} \end{bmatrix} \sim \mathrm{N}\left\{ \begin{bmatrix} 0 \\ 0 \end{bmatrix}, \psi_i = \begin{pmatrix} 0.0704 & -0.0507 \\ -0.0507 & 0.0415 \end{pmatrix} \right\}$$
$$\varepsilon_{ij} \sim \mathrm{N}(0, R_{ij} = 0.1052 G_{ij}^{0.5} \Gamma_{ij} G_{ij}^{0.5}), G_{ij} = \exp(0.0732 y_i), \Gamma_{ij} = I_{ni}$$

$$\mathrm{CL}_{ijk} = (1.3129 + v_{1ij})\mathrm{DBH}^{[0.1669+v_{1i}+(0.3562+v_{2ij})\mathrm{OP}]} + \varepsilon_{ijk} \quad (17)$$

where

$$v_i = \left[v_{1i}\right] \sim \mathrm{N}\{[0], \psi_i = (0.0029)\}$$
$$v_{ij} = \begin{bmatrix} v_{1ij} \\ v_{2ij} \end{bmatrix} \sim \mathrm{N}\left\{ \begin{bmatrix} 0 \\ 0 \end{bmatrix}, \psi_i = \begin{pmatrix} 0.0555 & -0.0164 \\ -0.0620 & 0.0057 \end{pmatrix} \right\}$$
$$\varepsilon_{ijk} \sim \mathrm{N}(0, R_{ij} = 0.6124 G_{ij}^{0.5} \Gamma_{ij} G_{ij}^{0.5}), G_{ij} = \exp(0.0958 y_i), \Gamma_{ij} = I_{ni}$$

3.4 Model prediction and evaluation

The results of L.Ratio (Table 10) indicated that in comparison to Eq. (10) and Eq. (12), the addition of random parameters in Eq. (16) could significantly improve the predictive ability for crown width. A similar improvement for crown length can also be found in Eq. (17) relative to Eq. (11) and Eq. (13). In addition, these improvements were reflected by NMSE and PRESS of the ten-fold cross-validation. Figure 8 also showed that the final models were unbiased, and model fits were good.

4 Discussion

We found that including CIs as predictor variables could significantly improve the performance of CW—DBH and CL—DBH basic models (Tables 6 and 7). The first hypothesis proposed in the Introduction was therefore accepted. Similar results were reported by Sharma et al. (2016), Thorpe et al. (2010), and Davies and Pommerening (2008), all who suggested that competition could significantly affect crown dimension and should be included into crown models. The CIs are comprehensive indicators describing the competition

Table 10 Comparisons among optimum basic model, optimum basic model with optimum competition index and optimum mixed-effects model for crown width and length, respectively

Equation	Adjust R^2	−2LL (df)	AIC	BIC	Test	L.Ratio	*p* value	NMSE	PRESS
(10)	0.4620	2552.41 (3)	2558	2574				0.5505	48.4941
(12)	0.5517	2211.93 (4)	2220	2241	(12) vs. (10)	340.48	< 0.0001	0.4390	38.7194
(16)	0.7469	1548.54 (9)	1567	1614	(16) vs. (12)	663.39	< 0.0001	0.2651	23.3120
(11)	0.4900	5346.14 (3)	53,527	5368				0.5302	332.3337
(13)	0.5724	5119.63 (4)	5128	5149	(12) vs. (14)	226.51	< 0.0001	0.4559	285.3949
(17)	0.6301	4780.25 (9)	4798	4846	(14) vs. (18)	339.38	< 0.0001	0.3861	221.7118

Adjust R^2, adjusted coefficient of determination; *−2LL (df)*, −2 log-likelihood (degree of freedom); *AIC*, Akaike information criterion; *BIC*, Bayesian information criterion; *Test*, likelihood ratio test; *L.Ratio*, the value of likelihood ratio test; *NMSE*, normalized mean square error; *PRESS*, predicted the error sum of squares

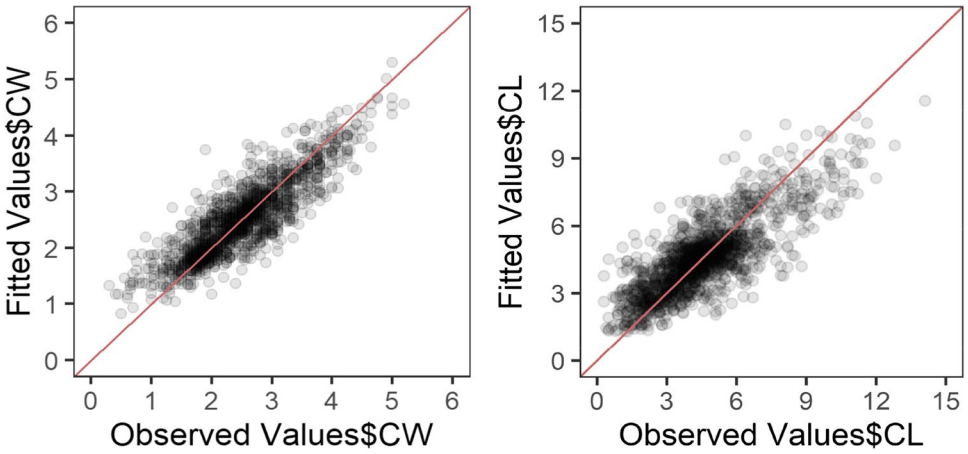

Fig. 8 Plots of predicted values against observed values of the final models

status of individual trees and hence can well represent an individual tree's space occupation and allocation of resources (light, water, or nutrients), which in turn determines growth (Kahriman et al. 2018). In addition to CW and CL models, CIs have been extensively used to develop individual-tree growth models. Many authors (Brand 2011; Collet and Chenost 2006) have found individual-tree growth models including CIs could provide for more accurate estimation.

The distance-dependent competition index, Alem, performed best in modeling the CW—DBH relationship (Table 6). Similarly, the distance-dependent competition index, OP, showed best performance in the CL—DBH model (Table 7). Our second hypothesis, i.e., the distance-dependent CIs perform better than distance-independent CIs for CW—DBH and CL—DBH relationship, was also accepted, which suggested that the distance-dependent CIs more appropriately and adequately describe competitive situations among individual trees in a stand than the distance-independent ones (Contreras et al. 2011; Sharma et al. 2016). Therefore, the interactions of the trees in a spatial manner over the restricted distances is essential for growth dynamics of the tree crowns. Many authors have also documented that distance-dependent CIs are superior to distance-independent ones, especially in mixed-species stands (Contreras et al. 2011; Quinonez-Barraza et al. 2018; Sharma et al. 2016). Additionally, the model showed that CW significantly increases with increasing Alem (Fig. 9). Alem, proposed by Alemdag (1978), is an index defined on the basis of the growing space for the subject tree (Burkhart and Tomé 2012). Therefore, trees with higher Alem or trees with larger growing space and area potentially available is expected to have larger crown sizes. OP was significantly positively related to CL (Fig. 9). Since OP reflects the degree to which the subject tree in the spatial structural unit is not shaded by competitor trees (Hu 2020). OP is an indicator of individual-tree light environment status in a forest stand and its relationship with CL suggested that trees with larger OP have stronger competitive ability for light which is considered as the major limiting resource for individual-tree growth. Therefore, a high OP will increase light supply, light capture, and light use efficiency, resulting in a larger crown.

A disadvantage of distance-dependent competition index is that it requires tree attributes and tree locations, which are expensive and labor intensive to acquire. However, with the

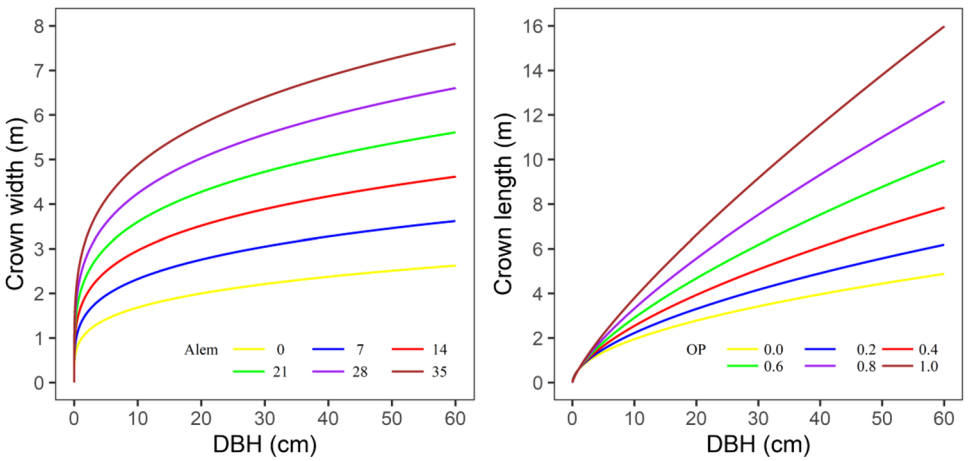

Fig. 9 Effect of competition indices on the crown width or length respectively for Chinese fir. The curves were produced using parameter estimates of optimum basic models with optimum competition index [Eqs. (12–13)]

development of remote sensing and geographic information systems (such as Light Detection and LiDAR) have facilitated the acquisition of tree-level spatial and dimensional data for the entire stands (Packalen and Maltamo 2006; Rowell 2009; Suratno et al. 2009), and are increasingly being used for forest and natural resource applications (Contreras et al. 2011; Suratno et al. 2009). The crown width and length models that depend on DBH and distance-dependent CIs in this study can be easily integrated with LiDAR inventory data and will be a useful tool to evaluate the influences of alternative management measures over time.

Except DBH and the competition index, which affect the crown width and length significantly, the crown structure is also largely influenced by site index, which is the most widely used measures of potential forest productivity and has strongly piratical utilized as a key input to both forest processes-based models and empirical growth and yield models (Amponsah et al. 2004; Fish et al. 2011; Yang 1998). Therefore, in this study, the SI was calculated respectively for the 16 sample plots by SI model (base age 20) developed by Duan and Zhang (2004) for the Chinese fir plantation to estimate the site quality. Unfortunately, because the results were not significant, and the site index was not left in the model. It might be attributed to the small study area, resulting in little difference in site quality. Additionally, many authors included other stand- or individual tree-level variables to model crown structure. For instance, Fu et al. (2017) evaluated 18 variables, including stand age [*A* (years)], height [*H* (m)], height to crown base [HCB (m)], site index [SI (m)], plot dominant height [DH (m)], and total diameter [LDTD (cm)]; four variables, i.e., DBH, DH, HCB, and *H*, were left the final model. For our model, we did not include other variables because more independent variables would reduce model generality (Hasenauer 2006; Vanclay 1994). Furthermore, additional independent variables also entail more labor and time, making data collection more expensive. Additionally, more independent variables impact model convergence and computational speed of parameter estimation (Montgomery et al. 1982).

Generality, precision, and reality are three important properties of a model that researchers strive to maximize (Levins 1966). However, Levins (1966) argued one of the three properties has to be sacrificed in order to achieve a higher level of the other two. Normally, many models have sacrificed generality to enhance reality and precision (Burkhart and Tomé 2012). Burkhart and Tomé (2012) documented that there is an increased interest in improving generality of models in the context of rapidly changing management and environmental conditions. In our study, we only included two variables to model CW and CL to enhance generality.

We produced two-level nonlinear mixed-effects models for predicting CW and CL. The performance of models significantly improved after introducing random effects. For instance, in comparison to the optimum fixed-effects CW model [Eq. (12)] and CL model [Eq. (13)], the AIC of the optimum mixed-effects models for CW and CL dropped by 653 and 330 respectively, and the adjusted R^2 increased by 0.1952 and 0.0577. Moreover, the model prediction and evaluation using the tenfold cross-validation further supported the conclusion that the mixed-effects approach had significantly improved the models' predictive performance. NMSE and PRESS were significantly reduced. The advantage of using a mixed-effects modeling approach to model crown structure has been also documented by other authors (Fu et al. 2013, 2017; Sharma et al. 2016). For instance, using a nested, two-level nonlinear mixed-effects approach, Fu et al. (2013) improved the prediction accuracy of crown width by including a site index and sample plot as random effects.

Mixed-effects models are tools used to deal with repeated measures and spatially-correlated data (Pinheiro and Bates 2006). Many authors documented that introducing random effects could correct or reduce autocorrelation and heteroscedasticity (Hasenauer 2006; Montgomery et al. 1982; Pommerening and Stoyan 2006; Wang et al. 2016). A similar result was found in our study. In addition, we further introduced three variance functions to refine our model. Finally, based on the lack-of-fit statistics, the exponent function was determined as the optimum option for reducing the heteroscedasticity of the residuals. Similar results were also reported by Zhao et al. (2013), Calama and Montero (2005) and Wang et al. (2019).

Determining parameters is of great importance when developing a mixed-effects model (Calama and Montero 2005). In previous studies, a common approach has been to first determine parameter effects and then incorporate additional predictor variables as fixed effects into a model (Budhathoki et al. 2008; Calama and Montero 2005). The additional predictor variables could introduce random effects (Fu et al. 2017), which often was not accounted for in previous studies. In this study, we determined parameter effects after including CIs in the models, and the random effects that the CIs introduced could be therefore be well represented.

The traditional method of computing CIs, we applied in this study, migth result in significant bias on the predicted variable of interest. Compared to the traditional method, more modern and more appropriate methods of computing CIs simultaneously with the model parameters have been used in a few studies, which can be able to describe competition impact on growth and development of individual-tree characteristics and produce more accurate output (Pommerening et al. 2011; Sharma and Brunner 2017). Therefore, the improving methods of computing CIs are strongly recommended in the future. Additionally, climate change has been reported to affect crown structure (Carnicer et al.

2011; Solberg 2004). For example, Carnicer et al. (2011) documented that drought resulting from climate change has a long-lasting chronic effect on crown structure, including increased crown defoliation rates for all tree species examined. It is imperative to integrate climatic variables into crown width and length models when data is available.

5 Conclusion

We produced CW and CL models using a two-level nonlinear mixed-effects approach. Our models showed that including CIs as predictor variables could significantly improve the performance of the models. Similarly, the second hypothesis, that distance-dependent CIs are superior to distance-independent ones when modeling CW and CL, was also supported. Compared with the CW and CL models with no random effects, the performance of the two-level nonlinear mixed-effects models improved. It is hoped that the final CW and CL models will contribute to the scientific management of the Chinese fir in other sites and under different environmental conditions.

Funding This research was funded by National Key R&D Program of China (grant number 2017YFC0505604).

Data availability The datasets generated during and/or analyzed during the current study are available from the corresponding author on reasonable request.

Declarations

Conflict of interest The authors declare that they have no conflict of interest.

References

Alemdag I (1978) Evaluation of some competition indexes for the prediction of diameter increment in planted white spruce. Forest Management Institute, Canada

Amponsah I, Lieffers V, Comeau P, Brockley R (2004) Growth response and sapwood hydraulic properties of young lodgepole pine following repeated fertilization. Tree Physiol 24:1099–1108

Bella I (1971) A new competition model for individual trees. For Sci 17:364–372

Biging G, Dobbertin M (1992) A comparison of distance-dependent competition measures for height and basal area growth of individual conifer trees. For Sci 38:695–720

Brand D (2011) A competition index for predicting the vigour of planted Douglas-fir in southwestern British Columbia. Can J for Res 16:23–29

Buba T (2013) Relationships between stem diameter at breast height (DBH), tree height, crown length, and crown ratio of *Vitellaria paradoxa* C.F. Gaertn in the Nigerian Guinea Savanna. Afr J Biotechnol 12:3441–3446

Budhathoki C, Lynch T, Guldin J (2008) Nonlinear mixed modeling of basal area growth for shortleaf pine. For Ecol Manag 255:3440–3446

Burkhart H, Tomé M (2012) Modeling forest trees and stands. Springer, Netherlands

Buschbacher R (1990) Natural forest management in the humid tropics: ecological, social, and economic considerations. Ambio 19:253–258

Calama R, Montero G (2004) Interregional nonlinear height–diameter model with random coefficients for stone pine in Spain. Can J for Res 34:150–163

Calama R, Montero G (2005) Multilevel linear mixed model for tree diameter increment in stone pine (*Pinus pinea*): a calibrating approach. Silva Fenn 39:37–54

Carnicer J, Coll M, Ninyerola M, Pons X, Sánchez G, Peñuelas J, Mooney H (2011) Widespread crown condition decline, food web disruption, and amplified tree mortality with increased climate change-type drought. Proc Natl Acad Sci USA 108:1474–1478

Carvalho J, Parresol B (2003) Additivity in tree biomass components of Pyrenean oak (*Quercus pyrenaica* Willd.). For Ecol Manag 179:269–276

Chen L, Sun Y, Saeed S (2018) Monitoring and predicting land use and land cover changes using remote sensing and GIS techniques—a case study of a hilly area, Jiangle, China. Plos One 13:e0200493

Chumachenko S, Korotkov V, Palenova M, Politov D (2003) Simulation modelling of long-term stand dynamics at different scenarios of forest management for coniferous–broad-leaved forests. Ecol Modell 170:345–361

Collet C, Chenost C (2006) Using competition and light estimates to predict diameter and height growth of naturally regenerated beech seedlings growing under changing canopy conditions. Forestry 79:489–502

Contreras M, Affleck D, Chung W (2011) Evaluating tree competition indices as predictors of basal area increment in western Montana forests. For Ecol Manag 262:1939–1949

Crookston N, Stage A (1999) Percent canopy cover and stand structure statistics from the Forest Vegetation Simulator. Gen. Tech. Rep. RMRSGTR-24. U.S. Department of Agriculture, Forest Service, Rocky Mountain Research Stationm Ogden, UT

Daniels R, Burkhart H, Clason T (1986) A comparison of competition measures for predicting growth of loblolly pine trees. Can J for Res 16:1230–1237

Davidian M (2017) Nonlinear models for repeated measurement data. Routledge, New York

Davies O, Pommerening A (2008) The contribution of structural indices to the modelling of Sitka spruce (*Picea sitchensis*) and birch (Betula spp.) crowns. For Ecol Manag 256:68–77

De Kort I, Loeffen V, Baas P (1991) Ring width, density and wood anatomy of Douglas fir with different crown vitality. IAWA J 12:453–465

Diggle P (2013) Statistical analysis of spatial and spatio-temporal point patterns. CRC Press, Boca Raton

Duan A, Zhang J (2004) Modeling of dominant height growth and building of polymorphic site index equations of Chinese fir plantation. Sci Silvae Sin 40:13–19

Fish H, Lieffers V, Silins U, Hall R (2011) Crown shyness in lodgepole pine stands of varying stand height, density, and site index in the upper foothills of Alberta. Can J for Res 36:2104–2111

Fu L, Sun H, Sharma R, Lei Y, Zhang H, Tang S (2013) Nonlinear mixed-effects crown width models for individual trees of Chinese fir (*Cunninghamia lanceolata*) in south-central China. For Ecol Manag 302:210–220

Fu L, Zhang H, Sharma R, Pang L, Wang G (2017) A generalized nonlinear mixed-effects height to crown base model for Mongolian oak in northeast China. For Ecol Manag 384:34–43

Gómez-Vázquez I, Fernandes P, Arias-Rodil M, Barrio-Anta M, Castedo-Dorado F (2014) Using density management diagrams to assess crown fire potential in *Pinus pinaster* Ait. stands. Ann for Sci 71:473–484

Geißler C, Nadrowski K, Kühn P, Baruffol M, Bruelheide H, Schmid B, Scholten T (2013) Kinetic energy of throughfall in subtropical forests of SE China – effects of tree canopy structure, functional traits, and biodiversity. Plos One 8:e49618

Grégoire T, Schabenberger O, Barrett J (1995) Linear modelling of irregularly spaced, unbalanced, longitudinal data from permanent-plot measurements. Can J for Res 25:137–156

Gregorie T (1987) Generalized error structure for forestry yield models. For Sci 33:423–444

Haase P (1995) Spatial pattern analysis in ecology based on Ripley's K-function: introduction and methods of edge correction. J Veg Sci 6:575–582

Hasenauer H (2006) Concepts within tree growth modeling. Springer, Berlin

Hegyi F (1974) A simulation model for managing jack-pine stands. In: Fries J (ed) Growth models for tree and stand simulation. Research Notes 30. Department of Forest Yield Research, Royal College of Forestry, Stockholm, pp 74–90

Hernandez-Moreno J, Bayeur N, Coley H IV, Hughes N (2017) Clouds homogenize shoot temperatures, transpiration, and photosynthesis within crowns of Abies fraseri (Pursh.) Poiret. Oecologia 183:667–676

Hu Y (2010) Structure-based spatial optimization management model for natural uneven-aged forest. Chinese Academy of Forestry

Hui G, Gadow K (2003) Quantitative analysis of forest spatial structure. Science and Technology Press, Beijing

Jiang X, Qiu X (1994) Research into simple competitive index and growth model for *Cunninghamia lanceolata*. Journal of Fujian College of Forestry 14:195–200

Johann K (1982) Der A-Wert ein objektiver Parameter zur Bestimmung der Freistellungsstärke von Zentralbäumen. Sektion Ertragskunde DVFFVA, Weibersbrunn, pp 146–158

Johnson R (1997) A historical perspective of the Forest Vegetation Simulator. In Proc.: Forest Vegetation Simulator conference, Feb. 3–7, 1997, Tech, R., M. Moeur, and J. Adams (Comps.). USDA For. Serv. Gen. Tech. Rep. No. INT-373

Kahriman A, Şahin A, Sönmez T, Yavuz M (2018) A novel approach to selecting a competition index: the effect of competition on individual-tree diameter growth of Calabrian pine. Can J for Res 48:1217–1226

Leiterer R, Furrer R, Schaepman M, Morsdorf F (2015) Forest canopy-structure characterization: a data-driven approach. For Ecol Manag 358:48–61

Leites L, Robinson A, Crookston N (2009) Accuracy and equivalence testing of crown ratio models and assessment of their impact on diameter growth and basal area increment predictions of two variants of the Forest Vegetation Simulator. Can J for Res 39:655–665

Levi R, Schaap M, Rasmussen C (2015) Application of spatial pedotransfer functions to understand soil modulation of vegetation response to climate. Vadose Zo J 14:0

Levins R (1966) The strategy of model building in population biology. Am Sci 54:421–431

Lin Z, Cao L, Wu C, Hong W, Hong T, Hu X (2018) Spatial analysis of carbon storage density of mid-subtropical forests using geostatistics: a case study in Jiangle County, southeast China. Acta Geochim 37:90–101

Lindstrom M, Bates D (1990) Nonlinear mixed effects models for repeated measures data. Biometrics 46:673–687

Lorimer C (1983) Tests of age-independent competition indices for individual trees in natural hardwood stands. For Ecol Manag 6:343–360

Mailly D, Turbis S, Pothier D (2003) Predicting basal area increment in a spatially explicit, individual tree model: a test of competition measures with black spruce. Can J for Res 33:435–443

Mallinis G, Mitsopoulos I, Stournara P, Patias P, Dimitrakopoulos A (2013) Canopy fuel load mapping of Mediterranean Pine sites based on individual tree-crown delineation. Remote Sens 5:6461–6480

Marshall D, Gregory P, David W (2003) Crown profile equations for stand-grown western hemlock trees in northwestern Oregon. Can J for Res 33:2059–2066

Martin G, Ek A (1984) A comparison of competition measures and growth models for predicting plantation red pine diameter and height growth. For Sci 30:731–743

Martin N, Chappelka A, Loewenstein E, Keever G, Somers G (2012) Predictive open-grown crown width equations for three oak species planted in a southern urban locale. Arboricult Urban For 38:58–63

Meng J, Li S, Wang W, Liu Q, Xie S, Ma W (2016a) Estimation of forest structural diversity using the spectral and textural information derived from SPOT-5 satellite images. Remote Sens 8:125

Meng J, Li S, Wang W, Liu Q, Xie S, Ma W (2016b) Mapping forest health using spectral and textural information extracted from SPOT-5 satellite images. Remote Sens 8:719

Meng S, Huang S (2009) Improved calibration of nonlinear mixed-effects models demonstrated on a height growth function. For Sci 55:238–248

Montgomery D, Peck E, Vining G (1982) Introduction to linear regression analysis. John Wiley & Sons, New York

Nagel J, Schmidt M (2006) The silvicultural decision support system BWINPro. Springer, Berlin

Pacala S, Canham C, Saponara J, Silander J, Kobe R, Ribbens E (1996) Forest models defined by field measurements: estimation, error analysis and dynamics. Ecol Monogr 66:1–43

Packalen P, Maltamo M (2006) Predicting the plot volume by tree species using airborne laser scanning and aerial photographs. For Sci 52:611–622

Pinheiro J, Bates D (2006) Mixed-effects models in S and S-PLUS. Springer Science & Business Media, New York

Pinheiro J, Bates D, Debroy S, Sakar D (2012) The nlme package: linear and nonlinear mixed effects models. R package version 3. Available: https://www.CRAN.R-project.org/package=nlme. Accessed July 2019

Pommerening A (2008) Analysing and modelling spatial woodland structure. Habilitationsschrift (DSc dissertation), University of Natural Resources and Applied Life Sciences, Vienna, Austria

Pommerening A, Lemay V, Stoyan D (2011) Model-based analysis of the influence of ecological processes on forest point pattern formation-a case study. Ecol Modell 222:666–678

Pommerening A, Stoyan D (2006) Edge-correction needs in estimating indices of spatial forest structure. Can J for Res 36:1723–1739

Pretzsch H, Biber P, Ïurský J, Sodtke R (2006) The individual-tree-based stand simulator SILVA. Springer, Berlin

Pukkala T, Becker P, Kuuluvainen T, Oker-Blom P (1991) Predicting spatial distribution of direct radiation below forest canopies. Agr for Meteorol 55:295–307

Pukkala T, Kolstroem T (1991) Effect of spatial pattern of trees on the growth of a Norway spruce stand. Silva Fenn 25:117–131

Purves D, Lichstein J, Pacala S (2007) Crown plasticity and competition for canopy space: a new spatially implicit model parameterized for 250 north American tree species. Plos One 2:e870

Quan N (1988) The prediction sum of squares as a general measure for regression diagnostics. J Bus Econ Stat 6:501–504

Quinonez-Barraza, Geronimo, Zhao D, Posadas D, Hector M, Corral-Rivas, Jose J (2018) Considering neighborhood effects improves individual dbh growth models for natural mixed-species forests in Mexico. Ann For Sci 75:1–11

Rüdiger G (2003) Estimation of crown radii and crown projection area from stem size and tree position. Ann for Sci 60:393–402

R Team RDC (2013) R: A language and environment for statistical computing. R foundation for statistical computing, Vienna. Austria Computing 14:12–21

Ritz C, Streibig J (2008) Nonlinear regression with R. Springer Science & Business Media, New York

Rouvinen S, Kuuluvainen T (1997) Structure and asymmetry of tree crowns in relation to local competition in a natural mature Scots pine forest. Can J for Res 27(6):890–902

Rowell E (2009) Estimating plot-scale biomass in a western North America mixed-conifer forest from lidar-derived tree stems. Proceedings of the Ninth International Conference on Lidar Applications for Assessing Forest Ecosystems. Texas A&M University, October 15, 2009

Russell M, Weiskittel A (2011) Maximum and largest crown width equations for 15 tree species in Maine. North J Appl for 28:84–91

Sánchez-González M, Viñas I, González G (2007) Generalized height-diameter and crown diameter prediction models for cork oak forests in Spain. For Syst 16:76–88

Sönmez T (2009) Diameter at breast height-crown diameter prediction models for *Picea orientalis*. Afr J Agric Res 4:214–219

Schröder J, Gadow K (1999) Testing a new competition index for Maritime pine in northwestern Spai. Can J for Res 29:280–283

Sharma R, Brunner A (2017) Modeling individual tree height growth of Norway spruce and Scots pine from national forest inventory data in Norway. Scand J for Res 32:501–514

Sharma R, Vacek Z, Vacek S (2016) Individual tree crown width models for Norway spruce and European beech in Czech Republic. For Ecol Manag 366:208–220

Sheather S (2009) A modern approach to regression with R. Springer, New York

Solberg S (2004) Summer drought: a driver for crown condition and mortality of Norway spruce in Norway. For Pathol 34:93–104

Stadt K, Huston C, Lieffers V (2002) A comparison of non-spatial and spatial, empirical and resource-based competition indices for predicting the diameter growth of trees in maturing boreal mixedwood stands. Sustainable Forest Management Network, G208 Biological Sciences Building, University of Alberta, Edmonton, Alberta

Stenberg P, Kuuluvainen T, Kellomäki S, Grace J, Jokela E, Gholz H (1994) Crown structure, light interception and productivity of pine trees and stands. Ecol Bull 43:20–34

Steneker G, Jarivis J (1963) A preliminary study to assess competition in a White Spruce-Trembling Aspen stand. For Chron 39:334–336

Suratno A, Seielstad C, Queen L (2009) Tree species identification in mixed coniferous forest using airborne laser scanning Isprs. J Photogramm Remote Sens 64:683–693

Tang M, Chen Y, Shi Y, Zhou G, Zhao M (2007) Intraspecific and interspecific competition analysis of community dominant plant populations based on Voronoi diagram. Acta Ecol Sin 27:4707–4716

Thorpe H, Astrup R, Trowbridge A, Coates K (2010) Competition and tree crowns: a neighborhood analysis of three boreal tree species. For Ecol Manag 259:1586–1596

Vanclay J (1994) Modelling forest growth and yield: applications to mixed tropical forests. CAB International, Wallingford

Vasilescu M (2013) Standard error of tree height using vertex III. Bulletin of the Transilvania University of Brasov, Series II: Forestry, Wood Industry, Agricultural Food Engineering 6:75–80

Vonesh E, Chinchilli V (1997) Linear and nonlinear models for the analysis of repeated measurements. J Biopharm Stat 18:595-610(516)

Wang H, Zhang G, Hui G, Li Y, Hu Y, Zhao Z (2016) The influence of sampling unit size and spatial arrangement patterns on neighborhood-based spatial structure analyses of forest stands. For Syst 25:e056

Wang W, Chen X, Zeng W, Wang J, Meng J (2019) Development of a mixed-effects individual-tree basal area increment model for oaks (*Quercus* spp.) considering forest structural diversity. Forests 10:474

Wang Y, Jarvis P (1990) Influence of crown structural properties on PAR absorption, photosynthesis, and transpiration in Sitka spruce: application of a model (MAESTRO). Tree Physiol 7:297–316

Warfield J (2006) An introduction to systems science. World Scientific, Singapore

Yang CR (1998) Foliage and stand growth responses of semimature lodgepole pine to thinning and fertilization. Can J for Res 28:1794–1804

Zarnoch S, Bechtold W, Stolte K (2004) Using crown condition variables as indicators of forest health. Can J for Res 34:1057–1070

Zeng W (2015) Modeling crown biomass for four pine species in China. Forests 6:433–449

Zhao L, Li C, Tang S (2013) Individual-tree diameter growth model for fir plantations based on;multi-level linear mixed effects models across southeast China. J for Res-JPA 18:305–315

Authors and Affiliations

Wenwen Wang[1] · Fangxing Ge[1,2] · Zhengyang Hou[1] · Jinghui Meng[1]

✉ Jinghui Meng
jmeng@bjfu.edu.cn

Wenwen Wang
wangwenwen_0321@163.com

Fangxing Ge
ge_fangxing@163.com

Zhengyang Hou
hou.zhengyang@gmail.com

[1] Research Center of Forest Management Engineering of National Forestry and Grassland Administration, Beijing Forestry University, Beijing 100083, China

[2] Jilin Forest Fire Brigade, Forest Fire Bureau of MEM, Changchun 130022, China